

Exploring confinement by cooling: A study of compact three-dimensional QED

Howard D. Trottier

Department of Physics, Simon Fraser University, Burnaby, British Columbia, Canada V5A 1S6

R. M. Woloshyn

TRIUMF, 4004 Wesbrook Mall, Vancouver, British Columbia, Canada V6T 2A3

(Received 24 May 1993)

The role of monopoles in the confining behavior of compact lattice three-dimensional QED (QED_3) is studied using an adiabatic cooling method. Monopole-antimonopole pairs with a large separation survive cooling and presence or absence of such plasma monopoles provides a useful classification of the lattice gauge-field configurations at large β . By calculating observables in subsets of gauge-field configurations which contain or do not contain plasma monopoles it is seen that, in compact QED_3 , monopoles dominate the long-distance physics, e.g., the string tension, linear confining potential, and dynamical mass generation. On the other hand, the spin-spin interaction is essentially unaffected by monopoles.

PACS number(s): 11.15.Ha, 11.15.Tk

I. INTRODUCTION

The cooling method was first proposed as a way of exposing topological configurations in lattice field theory [1,2]. More recently there has been a lot of discussion about cooling as a probe of confinement dynamics [3–8]. This was motivated by the finding of Campostrini *et al.* [3] that the string tension, i.e., the Creutz ratio of large Wilson loops, survives a significant amount of cooling. This invites a semiclassical interpretation for the confinement mechanism, a theme that was carried over to a study of quantum chromodynamics (QCD) in 2+1 dimensions by Duncan and Mawhinney [6,7]. However, precisely what cooling tells us about the confinement mechanism is still not completely clear. Teper [9] has argued that the local nature of the cooling algorithm inevitably leads to persistence of long-distance effects and does not necessarily reveal the underlying dynamics.

To gain some insight into how cooling can be used to explore confinement it seems reasonable to study a theory in which the confinement mechanism is well understood. In this paper we focus on compact quantum electrodynamics in 2+1 dimensions (QED_3). In this theory there is a semiclassical picture of confinement [10,11,7]. The instantons of this theory [which nonetheless are called monopoles due to their similarity to magnetic monopoles in (3+1)-dimensional theories] condense in the vacuum [10,11], producing a “magnetic” superconductor which confines electric flux. In the lattice QED_3 it is found that monopole-antimonopole pairs which are separated by more than a few lattice spacings (unbound or plasma monopoles as we will call them) survive local adiabatic cooling (see also Ref. [7]). The calculations reported here were done at weak coupling (large β) where the density of plasma monopole-antimonopole pairs is small and they are even absent in some of the gauge-field configurations produced by the Monte Carlo simulation. Then by calculating monopole properties in some detail

and comparing observables in gauge-field configurations with and without plasma monopoles, one sees quite clearly the role of monopoles in determining the long-distance behavior of the theory.

Section II contains a description of the calculational methods used in this paper. The single plaquette action is used to describe compact QED_3 . Gauge-field configurations were generated using the heat bath algorithm. With periodic boundary conditions it can happen that a monopole and antimonopole can annihilate leaving “magnetic” flux wrapped around the lattice. Once this happens such configurations are very difficult to change with local updating [12] so following Ref. [13] a global Metropolis update which injects a flux loop is done periodically to move the system in the space of field configurations.

Cooling was carried out using an algorithm that allows only a small local change in the gauge field at any step [3]. Monopole-antimonopole pairs with a small separation usually annihilate quite quickly (in terms of cooling sweeps). After about 20 cooling sweeps the monopoles become essentially static. Pairs that have a large separation have no chance of annihilating and further cooling evolves these configurations to some constant nonzero action. For QED_3 it is possible therefore to classify gauge-field configuration according to whether or not they contain monopoles or antimonopoles that survive cooling.

The observables calculated are the string tension and static potential obtained from Wilson loops, magnetic-field correlations which are related to the spin-spin interaction and the chiral-symmetry-breaking order parameter for staggered fermions. The results are given in Sec. III. The behavior of Wilson loops has some similarity with what was found in QCD. Small Wilson loops cool much more rapidly than large loops. The Creutz ratios of large loops do not change much under cooling so the string tension survives with only a small decrease from the uncooled value. This effect is associated in QED_3

with the fact that plasma monopoles become frozen into the gauge configurations and has been noted previously by Duncan and Mawhinney [7].

We can see more directly how monopoles affect the long-distance behavior of QED₃ by considering the static potential. Separating our ensemble of gauge-field configurations into a sample that contains monopoles that survive cooling (plasma monopoles) and a sample in which all monopoles- antimonopole pairs have small separations and annihilate, it was found that the static potential for these two samples behaves quite differently at large distances, *even without any cooling*. Only in the sample with plasma monopoles is there any evidence of confining behavior.

In contrast with the static potential, magnetic-field correlations, which are related to the spin-spin interaction [14,15], are essentially the same in uncooled configuration with or without plasma monopoles. Cooling reveals that monopoles (recall that these are the instantons of compact QED₃) play a very minor role in the spin-spin interaction. Since it has been suggested that instantons of QCD are important in the spin-dependent potential of that theory [16–18], there is a natural application of the methods used here.

Finally, chiral symmetry breaking in (quenched) compact QED₃ was examined. Again by considering configurations with and without plasma monopoles evidence is presented which suggests that, on the lattice, the presence of widely separated monopole-antimonopole pairs dominates dynamical mass generation. A small part of the chiral symmetry breaking comes from bound monopoles or quantum fluctuation effects.

II. METHOD

The usual plaquette action

$$S = \beta \sum_{x, \mu > \nu} \{1 - \cos[\theta_{\mu\nu}(x)]\} \quad (1)$$

is used for compact QED₃. The quantity β is the dimensionless coupling constant $1/e^2$ in lattice units and the plaquette angle is

$$\theta_{\mu\nu}(x) = \theta_{\mu}(x) + \theta_{\nu}(x + \hat{\mu}) - \theta_{\mu}(x + \hat{\nu}) - \theta_{\nu}(x)$$

in terms of link variables. Periodic boundary conditions in all directions were used for the gauge field. Field configurations were constructed using a heat bath algorithm.

Compact lattice QED contains field configurations with nontrivial topology. In our (2+1)-dimensional Euclidean space these are instantons but we follow the conventional nomenclature and use the term monopoles since these instantons are also the lattice analogs of Dirac monopoles. A convenient definition of lattice monopoles is that of DeGrand and Toussaint [19]. The plaquette angles are written as

$$\theta_{\mu\nu}(x) = \bar{\theta}_{\mu\nu}(x) + 2\pi n_{\mu\nu}(x), \quad (2)$$

where the reduced plaquette angle $\bar{\theta}_{\mu\nu}(x) \in (-\pi, \pi]$. Summing the oriented reduced plaquette angles associat-

ed with elementary cubes of the lattice allows one to find the monopoles essentially by identifying those cubes which contain the end of a Dirac string. For a finite lattice with periodic boundary conditions the number of antimonopoles equals the number of monopoles. On a finite lattice it can also happen that a monopole and antimonopole can annihilate leaving a “magnetic” flux loop that winds around the lattice [12]. To cope with the possible metastability of such configuration Damgaard and Heller [13] suggested doing periodic global Metropolis updates which introduce random flux loops. We use this procedure here.

Field configurations generated by the heat bath Monte Carlo algorithm were cooled using a local cooling algorithm containing a parameter δ which controls the rate of cooling. Cooling reduces the action monotonically by replacing links one at a time. Consider some particular link, characterized by an angle, call it θ , which is to be updated. The local contribution to the action can be written as

$$\tilde{S} = \beta [1 - r \cos(\theta + \theta_s)], \quad (3)$$

where $re^{i\theta_s}$ is the sum of the “staples” of the plaquettes containing the link being updated. Clearly, $\theta \rightarrow \theta' = -\theta_s$ minimizes \tilde{S} . However, to control the rate of cooling we adopt the prescription

$$\theta \rightarrow \theta' = \theta + \Delta\theta, \quad (4a)$$

$$|\Delta\theta| = \min\{\delta, |\theta + \theta_s|\}, \quad (4b)$$

$$\text{sgn}\Delta\theta = -\text{sgn}(\theta + \theta_s). \quad (4c)$$

This is the U(1) analogue of the algorithm used by Camprostrini *et al.* [3]. In the numerical calculations, $\delta = 0.05$ was used as in Ref. [3].

The results presented in this paper were calculated using cooling sweeps in which links were updated in a fixed sequence. However, some tests were done to see if cooling links in a random way introduced any differences. It was found that for a given starting configuration, the final position of a “frozen-in” monopole or antimonopole might occasionally differ by one lattice site between sequential and random updating. Also, in rare configurations the monopole number differs after cooling due to the annihilation of one more or fewer monopole-antimonopole pairs using fixed versus random updating. However, this happens sufficiently infrequently that we expect ensemble averages over large samples to be unchanged.

The behavior of a number of observables was monitored under cooling. First, the Creutz ratio

$$C(R, T) = -\ln \frac{W(R, T)W(R-1, T-1)}{W(R-1, T)W(R, T-1)}, \quad (5)$$

where $W(R, T)$ denotes the R by T rectangular Wilson loop, can be used to determine the string tension. For large loops, which obey the area law, $C(R, R)$ gives the string tension directly. The potential $V(R)$ between static charges is also considered. It is calculated by extrapolating Wilson loops to large T :

$$V(R) = - \lim_{T \rightarrow \infty} \frac{1}{T} \ln W(R, T). \quad (6)$$

In addition to the confining central interactions Dirac fermions will also have spin-spin and spin-orbit interactions, even in two spatial dimensions. These can be calculated on the lattice [14]. In particular, the spin-spin interaction is related to magnetic field correlations (see Ref. [15] for a simple derivation). In two spatial dimensions the magnetic field has only one component related to F_{12} , the field strength tensor in the spatial directions. The magnetic-field correlation is then calculated using a Wilson loop (say in the X - T plane) with insertion of spatial plaquettes in the time legs as shown in the Fig. 1. Let $\langle B(0, t_1) B(R, t_2) \rangle$ denote the configuration average of the type illustrated in Fig. 1. The correlation function we calculate is

$$\frac{1}{T-1} \sum_{t_1=T/2, T/2 \pm 1} \sum_{t_2=1, T-1} \frac{\langle B(0, t_1) B(R, t_2) \rangle}{W(R, T)}, \quad (7)$$

which, up to some (R -independent) factors, gives an estimate of the spin-spin interaction. In practice, the magnetic-field insertion B that was used was the average over the four spatial plaquettes whose corners lie on the Wilson loop $W(R, T)$ corresponding to operator II of Ref. [14].

Chiral symmetry breaking was also calculated. Staggered fermions were used with the usual action

$$S_f = \frac{1}{2} \sum_{x,u} \eta_\mu(x) [\bar{\chi}(x) e^{i\theta_\mu(x)} \chi(x+\hat{\mu}) - \bar{\chi}_{(x+\hat{\mu})} e^{i\theta_\mu(x)} \chi(x)] + \sum_x m \bar{\chi}(x) \chi(x) \quad (8a)$$

$$= \bar{\chi} M(\{\theta\}) \chi, \quad (8b)$$

where $\bar{\chi}, \chi$ are single component fermion fields, $\eta_\mu(x)$ is the staggered fermion phase [20] and m is the mass in lattice units. Antiperiodic boundary conditions were used for the fermion fields in all directions.

The chiral symmetry order parameter is calculated from the inverse of the fermion matrix M of Eq. (8b):

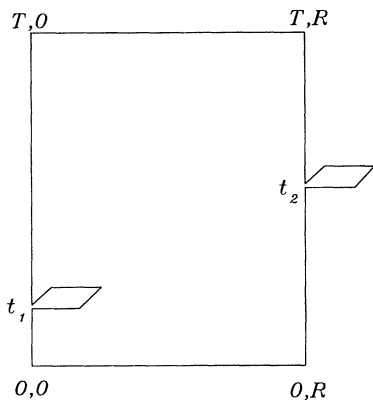


FIG. 1. Example of a Wilson loop with spatial plaquette insertions.

$$\langle \bar{\chi} \chi \rangle = \frac{1}{V} \langle \text{Tr} M^{-1}(\{\theta\}) \rangle, \quad (9)$$

where V is the lattice volume and the angular brackets denote the gauge-field configuration average. A random source method [21,22] was used to calculate $\text{Tr} M^{-1}(\{\theta\})$. Thirty-two Gaussian random sources were used for each gauge-field configuration.

III. RESULTS

The simulation was carried out at $\beta=2.5$ on a 20^3 lattice. This value of β was chosen so that a significant fraction of the configurations would have no monopoles after cooling.

After 5000 heat bath Monte Carlo sweeps to equilibrate, a total of 800 configurations, separated by 150 sweeps, were analyzed. The monopole number changes relatively slowly and 150 sweeps is roughly the autocorrelation time. Each configuration was cooled a total of 80 sweeps using the algorithm of Eq. (4) with $\delta=0.05$. The average plaquette $\langle \langle 1 - \cos \theta_{\mu\nu}(x) \rangle \rangle$ and the average number of monopoles N_m (recall number of anti-monopoles = number of monopoles) for the full sample of 800 configurations are plotted in Fig. 2 as a function of cooling sweeps. By about 30 cooling sweeps the average plaquette and monopole number have become essentially constant.

To better understand what is happening one needs more information about the monopole excitations in the

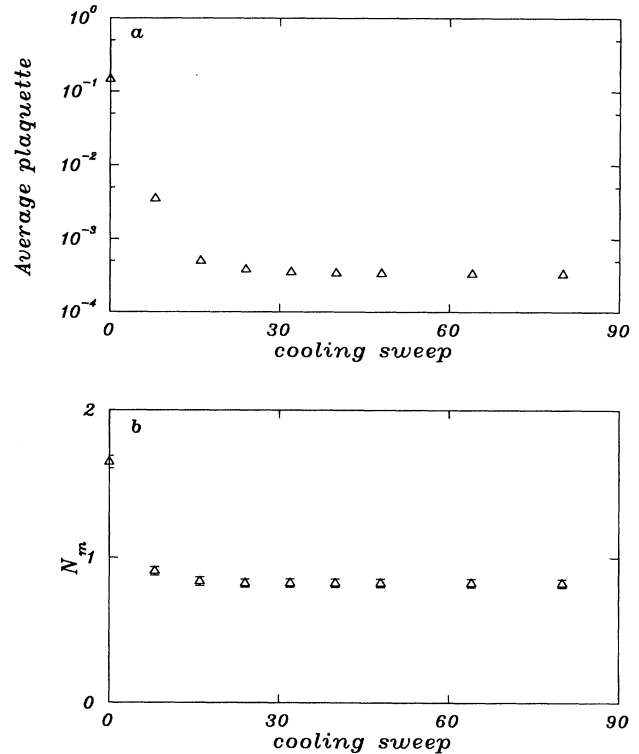


FIG. 2. (a) Average plaquette and (b) number of monopoles N_m as a function of a cooling sweep for the full sample of 800 configurations.

vacuum. This is provided in Fig. 3. The monopole-antimonopole correlation parameter C_m counts the number of times a monopole, located in an elementary cube on the lattice, has an antimonopole in a neighboring cube. From Fig. 3(a), it is seen that all "bound" monopole-antimonopole pairs, i.e., pairs on neighboring cubes, annihilate under cooling. Comparing C_m and N_m one sees that only a small fraction of the monopoles that are not initially in neighboring cubes annihilate. A more detailed examination of a few configurations showed that pairs separated by a distance greater than $\sqrt{3}$ lattice units, i.e., without a face, edge, or point in common, very rarely annihilate. This reflects the lack of mobility of the monopoles under slow local cooling. After cooling, what we call plasma monopoles are left. This is shown in another way in Fig. 3(b) where the average minimum separation between a monopole and the nearest antimonopole is plotted.

Figure 4 shows the Creutz ratio $C(R,R)$ for the full set of configurations with no cooling and with 16, 32, and 80 cooling sweeps. The features are the same as observed in previous calculations [3,7]. Small Wilson loops cool much more rapidly than large loops. The statistical fluctuations also decrease very rapidly making the string tension visible after a small amount of cooling. However, as also noted by Duncan and Mawhinney [7], the apparent string tension from slightly cooled configurations may be an overestimate of the true asymptotic string tension.

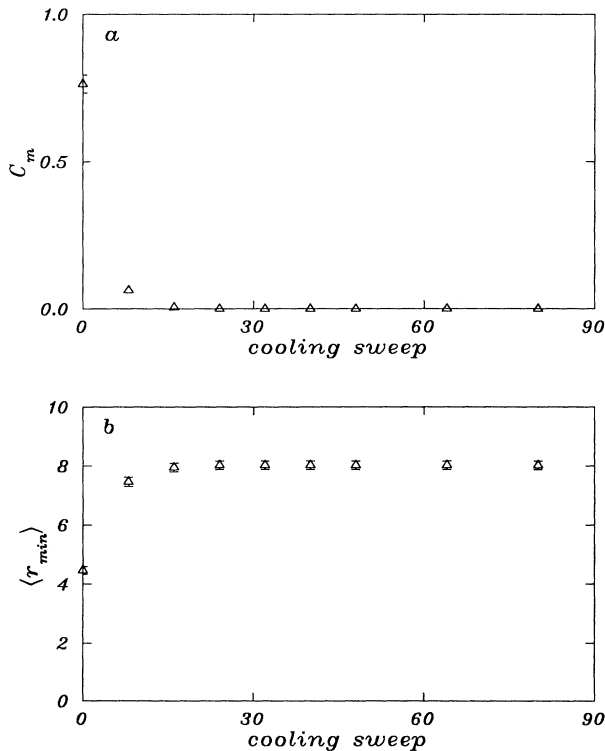


FIG. 3. (a) Number of neighboring monopole-antimonopole pairs C_m and (b) average minimum monopole-antimonopole separation $\langle r_{\min} \rangle$ as a function of a cooling sweep for the full sample of 800 configurations.

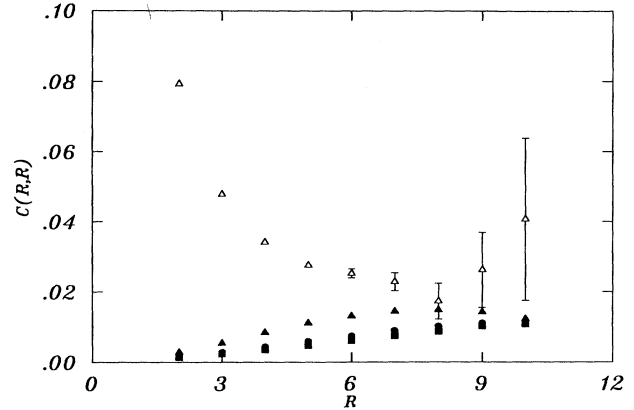


FIG. 4. The Creutz $C(R,R)$ as a function of loop size R for the full sample of 800 configurations with no cooling (Δ), 16 cooling sweeps (\blacktriangle), 32 cooling sweeps (\bullet), and 80 cooling sweeps (\blacksquare).

We would like to see the role of monopoles as directly as possible. Since at least some monopoles survive cooling it is natural to classify configurations according to whether they contain monopoles and antimonopoles after cooling ($N_m^c \neq 0$) or whether they do not ($N_m^c = 0$). Recall that configurations in which monopole-antimonopole pairs annihilate leaving flux wrapped around the lattice

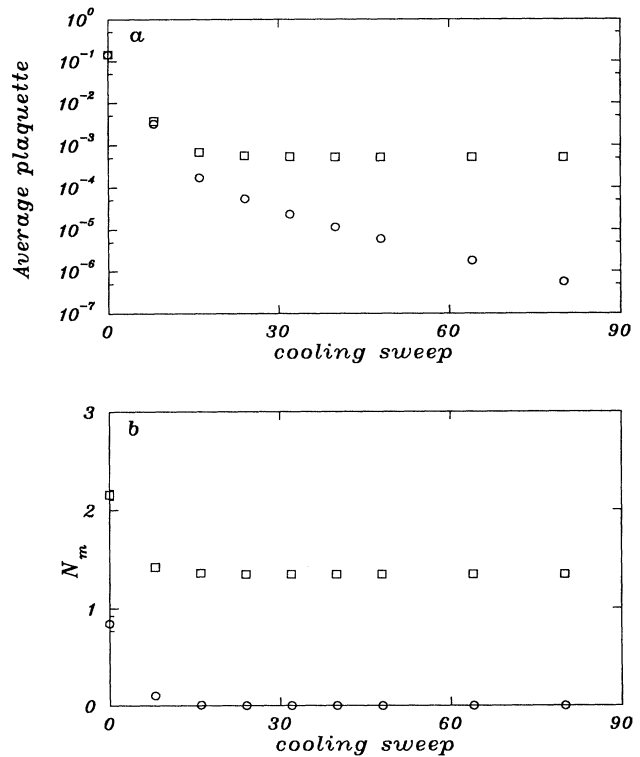


FIG. 5. (a) Average plaquette and (b) number of monopoles N_m as a function of a cooling sweep for the $N_m^c \neq 0$ sample of 488 configurations (\square) and the $N_m^c = 0$ sample of 145 configurations (\circ).

can occur. These are excluded from the $N_m^c=0$ sample. Out of a total 800 configurations, 488 went into the $N_m^c \neq 0$ sample and 145 had $N_m^c=0$.

The properties of the two samples, with and without monopoles that survive cooling, are compared in Figs. 5 and 6. Note, in particular, Fig. 6(b) which shows for the $N_m^c=0$ sample that it is essentially only monopole-antimonopole pairs separated by less than two lattice units that annihilate.

The Creutz ratio $C(R,R)$ for the $N_m^c=0$ and $N_m^c \neq 0$ ensembles are compared in Fig. 7 using uncooled configurations. Results with 16, 32, and 80 cooling sweeps are shown in Fig. 8. The large Wilson loops with no cooling are very noisy so a definitive statement is not possible but a trend is evident in Fig. 7: configurations without widely separated (plasma) monopole-antimonopole pairs show no sign of a string tension. With a small amount of cooling the situation becomes quite clear: without monopoles [Fig. 8(b)] large Wilson loops are not suppressed by an area law; i.e., the Creutz ratio becomes trivial. With monopoles [Fig. 8(a)], Wilson loops on the scale of the average monopole-antimonopole separation are suppressed and a string tension remains even with extreme cooling. Evidently with extreme cooling the string tension can be extracted from $C(R,R)$ only for R much larger than the average monopole-antimonopole separation.

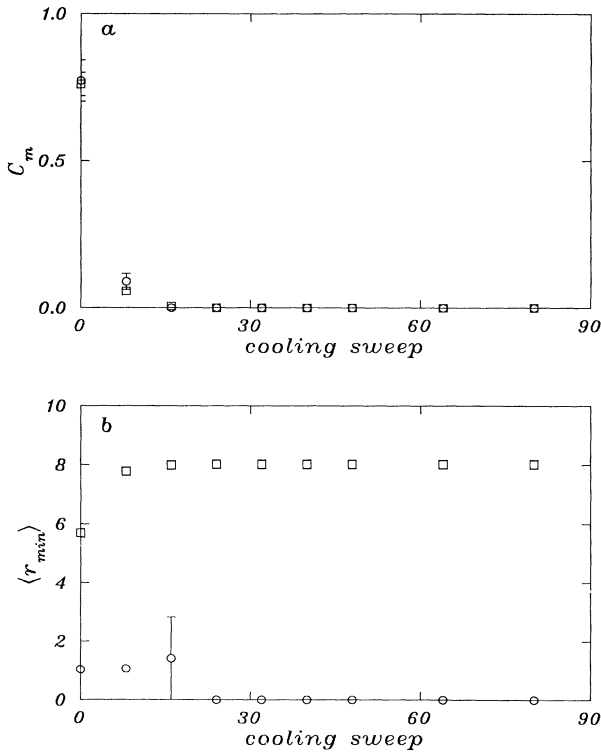


FIG. 6. (a) Number of neighboring monopole-antimonopole pairs C_m and (b) average minimum monopole-antimonopole separation $\langle r_{\min} \rangle$ as a function of a cooling sweep for the $N_m^c \neq 0$ sample of 488 configurations (\square) and the $N_m^c=0$ samples of 145 configurations (\circ).

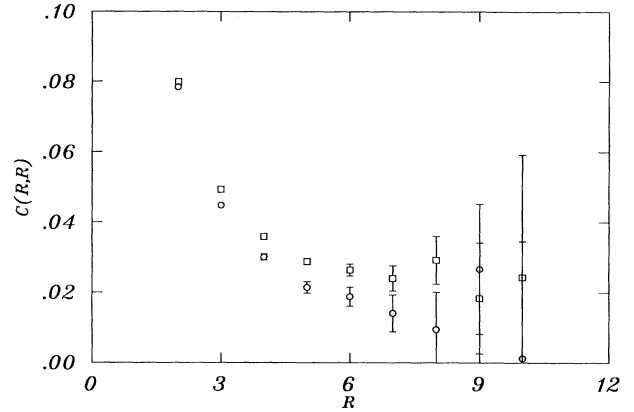


FIG. 7. The Creutz ratio $C(R,R)$ as a function of loop size R with no cooling for the $N_m^c \neq 0$ sample of 488 configurations (\square) and the $N_m^c=0$ sample of 145 configurations (\circ).

The above effect is seen even more nicely by considering the static potential directly. Figure 9 shows the static potential, Eq. (6), calculated using $N_m^c \neq 0$, $N_m^c=0$, and full uncooled gauge configuration samples. At short distances all potentials are the same suggesting that quantum fluctuations dominate [5]. However, the $N_m^c=0$ sample, from which plasma monopoles are excluded, yields a potential which shows a pronounced flattening at

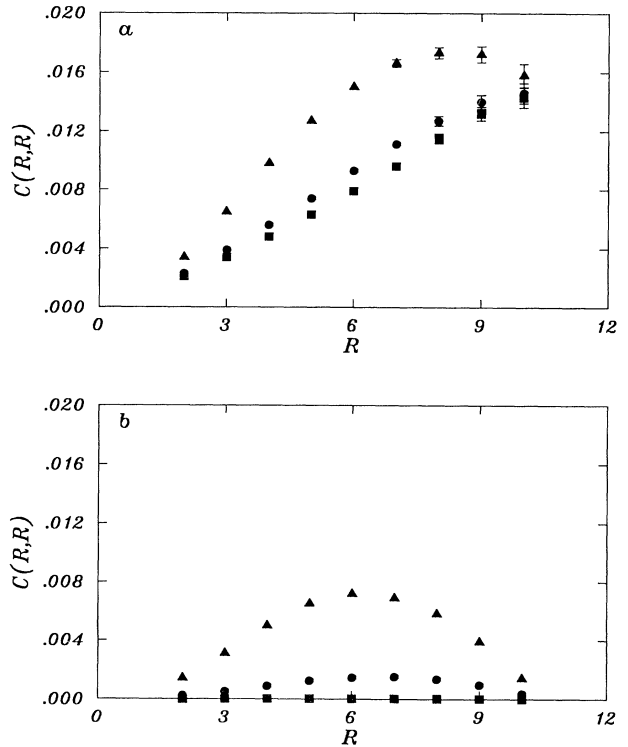


FIG. 8. The Creutz ratio $C(R,R)$ as a function of loop size R with 16 cooling sweeps (\blacktriangle), 32 cooling sweeps (\bullet), and 80 cooling sweeps (\blacksquare) (a) for the $N_m^c \neq 0$ sample and (b) for the $N_m^c=0$ sample.

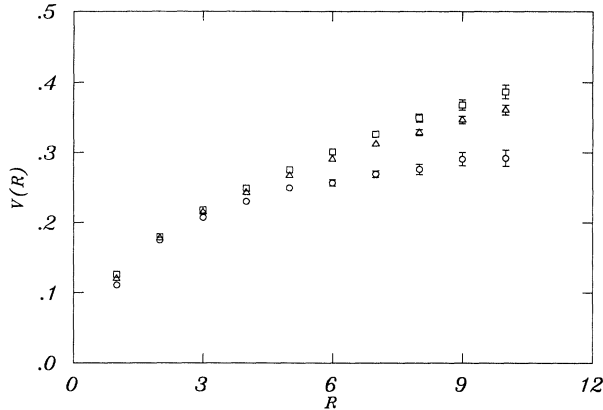


FIG. 9. The potential between static charges $V(R)$ versus separation R with no cooling for the full sample of 800 configurations (Δ), the $N_m^c \neq 0$ sample (\square), and the $N_m^c = 0$ sample (\circ).

large distance. After cooling the situation is shown in Fig. 10. The string tension extracted from the last few points of the uncooled $N_m^c \neq 0$ potential (open squares) is about 0.018 while after 80 cooling steps (solid squares) a string tension of about 0.013 is obtained. The Creutz ratio $C(R, R)$ [Fig. 8(a)] is apparently just in between which is reasonable since the potentials with cooled and uncooled configurations approach the limiting linear behavior with the opposite curvature [23].

In QCD we normally consider the spin-spin interaction as due to the exchange of gluons. However, there exist suggestions that a substantial part of the hyperfine interaction is due to instanton effects [16–18]. If this is so, we would expect magnetic-field correlations, which measure the spin-spin interaction [15], to be very different in configurations with different instanton properties. Also strong magnetic-field correlations would be expected to persist if instantons survive cooling. A calculation to test this directly has not yet been done for QCD (see however

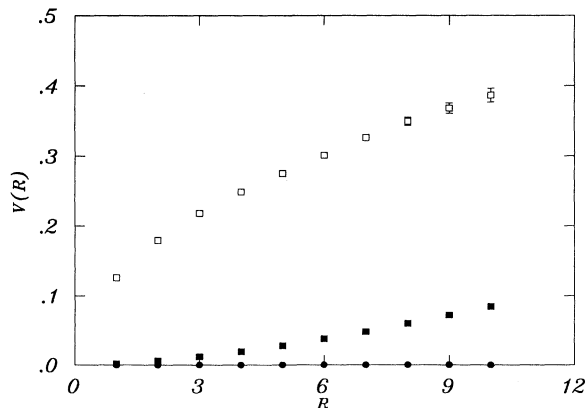


FIG. 10. The potential between static charges $V(R)$ versus separation R for the $N_m^c \neq 0$ sample with no cooling (\square) and after 80 cooling sweeps (\blacksquare). Also shown is the result for the $N_m^c = 0$ sample after 80 cooling sweeps (\bullet).

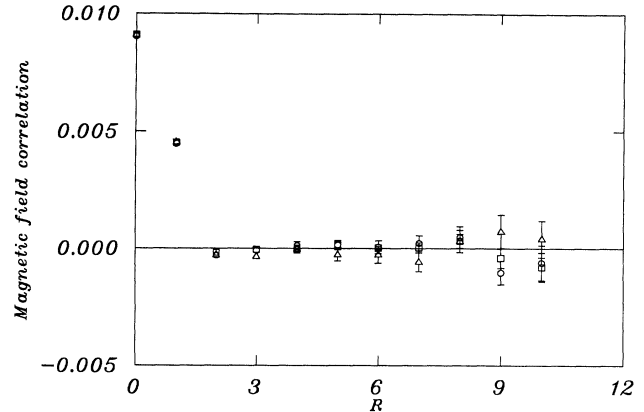


FIG. 11. The magnetic-field correlation (7) versus separation R with no cooling for the $N_m^c = 0$ sample (\square), a subset of the $N_m^c = 0$ configuration of the configurations which contain monopoles that annihilate when cooled (\circ), and a subset of the $N_m^c = 0$ configurations which contain no monopoles even before cooling (Δ).

Ref. [8]). For QED₃ the results are shown in Figs. 11 and 12. The squares in Fig. 11 show the magnetic-field correlation [Eq. (7)] calculated using the uncooled $N_m^c \neq 0$ gauge-field sample. The $N_m^c = 0$ sample was further divided into two sets of configurations: those which contain monopoles which annihilate under cooling and those configurations which contain no monopoles even before cooling. The magnetic-field correlation calculated with these two sets of uncooled configurations is shown in Fig. 11 by triangles and circles, respectively. Essentially no difference is discernible between the three calculations. Note also the magnetic-field correlation observed here is qualitatively the same as seen in QCD₄ (compare, for example, with the “operator II” results of Fig. 3 in Ref. [14]). Figure 12 shows the magnetic-field correlation for the $N_m^c \neq 0$ sample after 80 cooling sweeps (note the change in scale from Fig. 11). For QED₃ at least, monopoles (instantons) apparently play a very small role in the

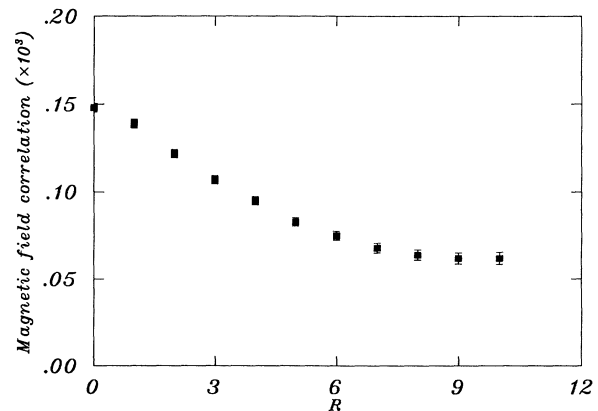


FIG. 12. The magnetic-field correlation (7) versus separation R after 80 cooling sweeps for the $N_m^c \neq 0$ sample.

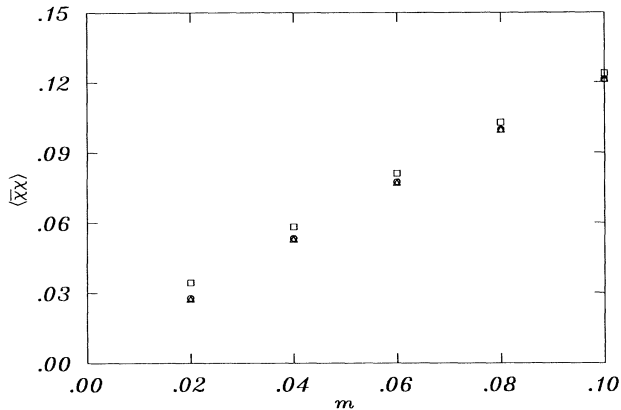


FIG. 13. The chiral order parameter $\langle \bar{\chi}\chi \rangle$ versus fermion mass m (in lattice units) with no cooling calculated for a subset of $N_m^c \neq 0$ configurations (\square) a subset of $N_m^c = 0$ configurations which contain monopoles that annihilate when cooled (\circ) and subset of $N_m^c = 0$ configurations which contain no monopoles even before cooling (\triangle).

spin-spin interaction which is due predominantly to short-distance quantum fluctuations.

In addition to linear confinement of charge, compact QED₃ has another property which is also important in QCD₄, namely, chiral symmetry breaking. It is natural to seek a common mechanism behind these two phenomena [24]. We calculated the chiral-symmetry-breaking parameter $\langle \bar{\chi}\chi \rangle$ for staggered fermions for a subset (400) of our quenched gauge-field configurations. The mass range for the calculations was 0.02–0.1 in lattice units. A nonzero value in the limit of zero fermion mass indicates chiral symmetry breaking. The results for uncooled configurations are shown in Fig. 13. As with the magnetic-field correlation it is instructive to consider three subsets of configurations: configurations containing monopoles after cooling ($N_m^c \neq 0$), configurations containing only monopoles that annihilate when cooled, and those with no monopoles at all. Figure 13 shows that the presence of plasma monopoles, which leads to linear confinement, also significantly enhances dynamical mass generation. Configurations containing monopole-antimonopole pairs separated only by short distances give essentially the same value of $\langle \bar{\chi}\chi \rangle$ as configurations that contain only nontopological quantum fluctuations. In the continuum limit, $\beta \rightarrow \infty$, monopole fluctuations disappear [19] but chiral symmetry breaking is expected to persist (see [25] and references therein). Our results are qualitatively consistent with this expectation. Determining a precise value for $\langle \bar{\chi}\chi \rangle$ at zero fermion mass is very difficult (see example Ref. [26]) but a qualitative conclusion, for example, by linearly extrapolating from the last few mass points in Fig. 13, is that $\langle \bar{\chi}\chi \rangle|_{m=0}$ is nonzero in all subsets of configurations; i.e., nontopological quantum fluctuation can give chiral symmetry breaking. At $\beta=2.5$ dynamical mass generation, however, seems to be dominated by plasma monopoles even though the density of such monopoles is not very large. After 80

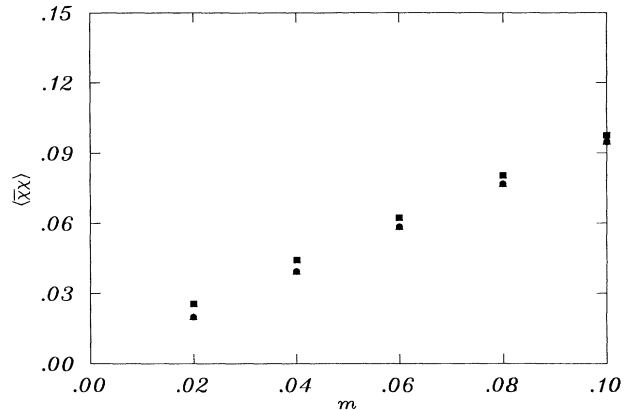


FIG. 14. The chiral order parameter $\langle \bar{\chi}\chi \rangle$ versus fermion mass m (in lattice units) after 80 cooling sweeps calculated for a subset of $N_m^c \neq 0$ configurations (\blacksquare), a subset of $N_m^c = 0$ configurations which contain monopoles that annihilate when cooled (\bullet) and a subset of $N_m^c = 0$ configurations which contain no monopoles even before cooling (\blacktriangle).

cooling surveys we get the results in Fig. 14. Chiral symmetry breaking persists in those configurations which contain plasma monopoles not annihilated under cooling.

IV. SUMMARY

In this paper we show how cooling can be used to correlate the long-distance confining behavior of compact QED₃ with the presence of separated monopole-antimonopole pairs in the vacuum. Such plasma monopoles survive cooling in QED₃ and therefore it is possible to use their presence as a way of classifying gauge-field configurations. The difference between our work and previous studies is that after determining the monopole properties by cooling we go back to recalculate and compare observables in subsets of gauge-field configuration with different long-distance monopole characteristics. What emerges is a consistent picture: the Creutz ratio $C(R, R)$ and the static potential $V(R)$ are determined at large R by the presence of monopole-antimonopole pairs with separation comparable to R . Cooling out quantum fluctuations or monopole-antimonopole pairs with small separation does not change the long-distance behavior appreciably.

Chiral symmetry breaking, which is also a long-distance phenomenon, was also seen to be dominated at $\beta=2.5$ by plasma monopoles. On the other hand, magnetic-field correlations which determine the spin-spin interaction seem to be determined by short-distance effects. After cooling, only a very small correlation from plasma monopoles remains.

Our study of QED₃ points to some calculations that can be done in QCD₄. Obviously instanton effects can be looked for in the same way as done here. However, there are other kinds of topological excitations that one may try to examine, for example, Abelian monopoles [27] or vortices [28]. These type of objects apparently do not get

frozen in under cooling [29] so some modification of our method would be necessary. However one lesson can be learned from the present study, that is, one needs to correlate the behavior of observables with more detailed vacuum properties rather than simply focusing on, for example, the monopole density as has been done in many papers up to now [29,30].

ACKNOWLEDGMENTS

One of us (R.M.W.) thanks T. Fujita and M. Oka for some helpful discussion. This work was supported in part by the Natural Sciences and Engineering Research Council of Canada.

-
- [1] B. Berg, *Phys. Lett.* **104B**, 475 (1981); Y. Iwasaki and T. Yoshie, *ibid.* **125B**, 197 (1983).
- [2] J. Hoek, *Phys. Lett.* **166B**, 199 (1986); M. Teper, *Phys. Lett. B* **171**, 86 (1986); E.-M. Ilgenfritz, M. L. Laursen, M. Müller-Preussker, G. Schierholz, and H. Schiller, *Nucl. Phys.* **B268**, 693 (1986).
- [3] M. Campostrini, A. Di Giacomo, M. Maggiore, H. Panagopoulis, and E. Viccari, *Phys. Lett. B* **225**, 403 (1989).
- [4] A. Di Giacomo, M. Maggiore, and Š. Olejnik, *Phys. Lett. B* **236**, 199 (1990).
- [5] M. Faber, H. Markum, M. Müller, and Š. Olejnik, *Phys. Lett. B* **247**, 377 (1990).
- [6] A. Duncan and R. Mawhinney, *Phys. Lett. B* **241**, 403 (1990).
- [7] A. Duncan and R. Mawhinney, *Phys. Rev. D* **43**, 554 (1991).
- [8] M.-C. Chu and S. Huang, *Phys. Rev. D* **45**, 2446 (1992).
- [9] M. Teper, in *Lattice '90*, Proceedings of the International Symposium, Tallahassee, Florida, 1990, edited by U. M. Heller, A. D. Kennedy, and S. Sanielevici [*Nucl. Phys. B (Proc. Suppl.)* **20**, 159 (1991)].
- [10] A. M. Polyakov, *Phys. Lett.* **59B**, 82 (1975); *Nucl. Phys.* **B120**, 429 (1977).
- [11] T. Banks, R. Myerson, and J. Kogut, *Nucl. Phys.* **B129**, 493 (1977).
- [12] V. Grösch, K. Jansen, J. Jersak, C. B. Lang, T. Neuhaus, and C. Rebbi, *Phys. Lett.* **162B**, 171 (1985).
- [13] P. H. Damgaard and U. M. Heller, *Nucl. Phys.* **B309**, 625 (1988).
- [14] C. Michael and P. E. L. Rakow, *Nucl. Phys.* **B256**, 640 (1985).
- [15] A. Katzouraki, *Z. Phys. C* **41**, 653 (1989).
- [16] M. A. Shifman, A. I. Vainshtein, and V. J. Zakharov, *Nucl. Phys.* **B163**, 46 (1980).
- [17] E. V. Shuryak and J. L. Rosner, *Phys. Lett. B* **218**, 72 (1989).
- [18] M. Oka and S. Takeuchi, *Phys. Rev. Lett.* **63**, 1780 (1989).
- [19] T. A. DeGrand and D. Toussaint, *Phys. Rev. D* **22**, 2478 (1980).
- [20] N. Kawamoto and J. Smit, *Nucl. Phys.* **B192**, 100 (1981).
- [21] R. Scalettar, D. Scalapino, and R. Sugar, *Phys. Rev. B* **34**, 7911 (1986); S. Gottlieb, W. Liu, D. Toussaint, R. L. Renken, and R. L. Sugar, *ibid.* **35**, 3972 (1987); K. Bitar, A. D. Kennedy, R. Horsley, S. Meyer, and P. Rossi, *Nucl. Phys.* **B313**, 348 (1989).
- [22] H. R. Fiebig and R. M. Woloshyn, *Phys. Rev. D* **42**, 3520 (1990).
- [23] An analytical expression for the string tension derived using the Villain action [10,11] gives $\sigma(\beta=2.5)=0.0125$. See R. J. Wensley and J. D. Stack, *Phys. Rev. Lett.* **63**, 1764 (1989). Our string tension using cooled configurations containing plasma monopoles is consistent with this value.
- [24] A. Casher, *Phys. Lett.* **83B**, 395 (1979).
- [25] D. C. Curtis, M. R. Pennington, and D. Walsh, *Phys. Lett. B* **295**, 313 (1992).
- [26] S. Hands and J. B. Kogut, *Nucl. Phys.* **B335**, 455 (1990).
- [27] G. 't Hooft, *Nucl. Phys.* **B190**, 455 (1981); A. Kronfeld, G. Schierholz, and U.-J. Wiese, *ibid.* **B293**, 461 (1987).
- [28] G. 't Hooft, *Nucl. Phys.* **B138**, 1 (1978); R. Mawhinney, *ibid.* **B321**, 653 (1989).
- [29] L. Del Debbio, A. Di Giacomo, M. Maggiore, and Š. Olejnik, *Phys. Lett. B* **267**, 254 (1991).
- [30] T. L. Ivanenko, A. V. Pochinsky, and M. I. Polikarpov, *Phys. Lett. B* **252**, 631 (1990); V. G. Bornyakov, E.-M. Ilgenfritz, M. L. Laursen, V. K. Mitryushkin, M. Müller-Preussker, A. J. van der Sijs, and A. M. Zadorozhny, *ibid.* **261**, 116 (1991); S. Hioki, S. Kitahara, S. Kiura, Y. Matsu- bara, O. Miyamura, S. Ohno, and T. Suzuki, *ibid.* **272**, 326 (1991).